

this and established an apparent  $K_I$  of 20  $\mu\text{M}$ .<sup>17</sup> Incubation of the enzyme with 250  $\mu\text{M}$  **2** for 45 min, followed by removal of the inhibitor, gives no recovery of activity.<sup>18</sup> Furthermore, treatment with 4 M urea and inhibitor removal also fails to restore activity,<sup>18</sup> thereby demonstrating that the inactivation is irreversible and probably not due to a slow-binding inhibitor with a high dissociation constant. Preincubation of PHM with substrate (D-Phe-L-Phe-Gly) (**1**) and **2** shows protection of the enzyme in proportion to the amount of added substrate, which indicates that **2** acts at the active site of the enzyme. Treatment of PHM with **2** in the absence of  $\text{Cu}^{\text{II}}$  and ascorbate for 1 h followed by removal of the inhibitor results in no significant loss of activity. The requirement that all cofactors be present for inactivation to occur illustrates that **2** is a mechanism-based inhibitor.

Possible mechanisms of action for **2** are depicted in Scheme II. Abstraction of the  $\alpha$ -hydrogen from the D-vinylglycine residue produces a conjugated radical at the  $\alpha$ -carbon. Direct hydroxylation (path A) would generate a vinylglycine carbinol amide that can cleave to give the peptide amide and the  $\alpha$ -keto acid, a potential alkylating species. Oxidative electron transfer (path B) could form a very reactive *N*-acyl iminium species that could result in the covalent attachment of the inhibitor to the enzyme. Path C involves interaction of the resonance-stabilized radical at the distal primary carbon with amino acid residues in the enzyme active site (e.g., hydrogen abstraction). To gain further insight, the inhibitor was resynthesized with a fluorescent 5-(dimethylamino)-1-naphthalenesulfonyl (dansyl) group attached to the amino terminus. Compound **5** also irreversibly inhibits PHM. A large sample of the enzyme was inactivated with this fluorescent tripeptide, a small amount of active PHM was then added to aid in isolation, and the inactivated enzyme was separated from **5** by gel filtration chromatography. Fractions containing amidating activity were pooled and concentrated as were those which had a UV absorption at 250 nm ( $\lambda_{\text{max}}$  of **5**). Spectrofluorimetric analysis of these samples showed no fluorescence associated with the PHM fractions above the minimum level of detection (ca. 5 pmol). A single late-eluting fraction which did fluoresce was further analyzed by HPLC and found to contain the tripeptide **5**.

These results indicate that the substrate analogues **2** and **5** inactivate PHM by a process that results in cleavage of the terminal portion of the peptide substrate (e.g., path A, Scheme II).<sup>19</sup> Current work on the detailed mechanism of this inactivation, along with studies on a variety of other inhibitors of PHM, will be described later.

**Acknowledgment.** We wish to thank Mr. Darrell Belke for assistance in acquiring the scanned fluorescence spectra and Professor Larry Wang for use of the SLM/Aminco 8000C spectrofluorimeter. Stimulating discussions with Dr. Arlindo Castelhan (Syntex Canada) are gratefully acknowledged. Financial support was provided by the Natural Sciences and Engineering Research Council of Canada, the Alberta Heritage Foundation for Medical Research, and postdoctoral fellowships from NATO (U. S. National Science Foundation) and the Killam Foundation to T.M.Z.

**Supplementary Material Available:** Schemes for the syntheses of compounds **2**–**5** (4 pages). Ordering information is given on any current masthead page.

(17) The enzyme was isolated as described previously.<sup>7a</sup> Preincubation mixtures (250  $\mu\text{L}$ ) contained 50  $\mu\text{L}$  of enzyme and varying amounts of **2** in a cocktail of 1 mM ascorbate, 5 mM  $\text{CuSO}_4$ , 25 mM KI, 0.125 mg/mL catalase, and 1 mg/mL BSA in 50 mM  $\text{Na}_2\text{HPO}_4/\text{NaH}_2\text{PO}_4$  and 200 mM NaCl, pH 6.8 buffer. Aliquots (25  $\mu\text{L}$ ) of the preincubated mixtures were diluted into 475- $\mu\text{L}$  solutions containing 1.26  $\mu\text{M}$  D-Phe-L-Phe-[1,2-<sup>14</sup>C]Gly (specific activity 113  $\mu\text{Ci}/\mu\text{mol}$ ) and 83  $\mu\text{M}$  unlabeled **1** ( $10 \times K_M$ ) in the same cocktail and incubated for 1 h. The percent of substrate converted was determined as described previously.<sup>9</sup>

(18) The inhibitor was removed by three dilution/concentration steps using an Amicon (Beverly, MA) Centricon-30 ultrafiltration device. Uninhibited PHM remains active during this procedure.

(19) Path B is also possible if cleavage of the *N*-acyl imine bond occurs.

## A Novel $\text{FeC}_{60}$ Adduct in the Solid State

T. Pradeep, G. U. Kulkarni, K. R. Kannan, T. N. Guru Row, and C. N. R. Rao\*

CSIR Centre of Excellence in Chemistry and  
Solid State and Structural Chemistry Unit  
Indian Institute of Science  
Bangalore 560 012, India

Received October 7, 1991

Revised Manuscript Received January 27, 1992

The 7-Å diameter cavity in buckminsterfullerene has long been considered as a possible host for various atoms and molecules.<sup>1</sup> There have been several attempts to incorporate metal atoms such as La into this cavity, and these studies<sup>2–6</sup> have mainly employed mass spectrometry for characterization. The question of whether the metal atom is inside or outside the spheroidal hollow cage in these species has not been fully resolved. Freiser and co-workers<sup>4</sup> have generated an  $\text{FeC}_{60}$  complex in the gas phase by means of a ligand-exchange reaction and have also characterized  $\text{NiC}_{60}$  and  $\text{Ni}(\text{C}_{60})_2$  in the gas phase. One example where an atom has been entrapped in  $\text{C}_{60}$  is that where a high-energy beam of  $\text{C}_{60}$  is made to interact with helium to give  $\text{HeC}_{60}$  in the gas phase.<sup>5</sup> Chai et al.<sup>6</sup> have recently prepared fullerenes with La trapped in the cages by laser vaporization. Metal complexes of  $\text{C}_{60}$  where the metal is present outside the cavity have been prepared by solution methods and characterized.<sup>7,8</sup> We investigated an iron adduct of  $\text{C}_{60}$ ,  $\text{FeC}_{60}$  (**I**), where iron atoms were introduced during the contact-arc vaporization of graphite, expecting that this would result in the entrapment of Fe in the cavity. In order to understand some of the unique features of this adduct, we have compared its properties with those of solid  $\text{FeC}_{60}$  (**II**), where Fe is clearly bound externally to the fullerene.

In our effort to obtain the Fe adduct of  $\text{C}_{60}$  with the metal inside the cage, we carried out the contact-arc vaporization of graphite in an atmosphere of  $\text{Fe}(\text{CO})_5$ . The arc chamber was pumped to a base vacuum of  $\sim 10^{-6}$  Torr, and He gas was admitted to about 50 Torr through a needle valve.  $\text{Fe}(\text{CO})_5$  was admitted to the system from a reservoir at the same rate as He. The soot<sup>9</sup> was washed with diethyl ether, the residue was Soxhlet-extracted with toluene for about 3 h, and the extract was vacuum-dried at 380 K to remove any volatile iron compounds. The mass spectrum of the product of solvent extraction<sup>10</sup> showed the presence of mass peaks other than those due to  $\text{C}_{60}$  and  $\text{C}_{70}$ , which could be ascribed to  $\text{FeC}_{60}$ . The sample showed an additional spot in the TLC other than those due to  $\text{C}_{60}$  and  $\text{C}_{70}$  with an  $R_f$  value close to that of  $\text{C}_{70}$ . After  $\text{C}_{60}$  was separated out by column chromatography, the new product was eluted along with a small proportion of  $\text{C}_{70}$ .

The mass spectrum of the new product (in mixture with  $\text{C}_{70}$ ) obtained after column chromatography (Figure 1) showed peaks at 776, 752, and 728, ascribable to  $\text{FeC}_{60}$ ,  $\text{FeC}_{58}$ , and  $\text{FeC}_{56}$ , besides peaks at 720 and 840;<sup>11</sup> a peak at 388 was seen due to

(1) Kroto, H. W.; Heath, J. R.; O'Brien, S. C.; Curl, R. F.; Smalley, R. E. *Nature* **1985**, *318*, 162.

(2) Heath, J. R.; O'Brien, S. C.; Zhang, Q.; Liu, Y.; Curl, R. F.; Kroto, H. W.; Tittel, F. K.; Smalley, R. E. *J. Am. Chem. Soc.* **1985**, *107*, 7779.

(3) Cox, D. M.; Trevor, D. J.; Reichmann, K. C.; Kaldor, A. *J. Am. Chem. Soc.* **1986**, *108*, 2457.

(4) Roth, L. M.; Huang, Y.; Schwedler, J. T.; Cassady, C. J.; Ben-Amotz, D.; Kahr, B.; Freiser, B. S. *J. Am. Chem. Soc.* **1991**, *113*, 6298. Huang, Y.; Freiser, B. S. *J. Am. Chem. Soc.* **1991**, *113*, 8186.

(5) Ross, M. M.; Callahan, J. H. *J. Phys. Chem.* **1991**, *95*, 5720.

(6) Chai, Y.; Guo, T.; Jin, C.; Haufler, R. E.; Chibante, L. P. F.; Fure, J.; Wang, L.; Alford, J. M.; Smalley, R. E. *J. Phys. Chem.* **1991**, *95*, 7568.

(7) Hawkins, J. M.; Meyer, A.; Lewis, T. A.; Loren, S.; Hollander, F. J. *Science* **1991**, *252*, 312.

(8) Fagan, P. J.; Calabrese, J. C.; Malone, B. *Science* **1991**, *252*, 1160.

(9) The <sup>57</sup>Fe Mössbauer spectrum of the soot showed 6-finger patterns attributable to magnetic  $\text{Fe}_3\text{C}$  and  $\alpha$ -Fe along with a singlet due to a new species.

(10) The mass spectrum of the residue left over after the solvent extraction did not show any volatile species up to 400 °C.

(11) An intense peak at  $m/z$  720 is found in the mass spectrum of pure  $\text{C}_{70}$  as well.

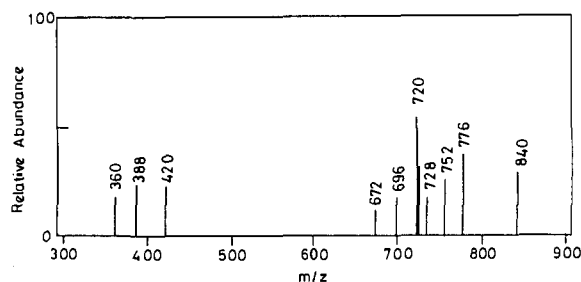


**Figure 1.** Mass spectrum of  $\text{FeC}_{60}$  (I) (in mixture with  $\text{C}_{70}$ ) from the gas-phase reaction. Peaks at 840, 720, 696, and 672 arise from the parent fullerenes.

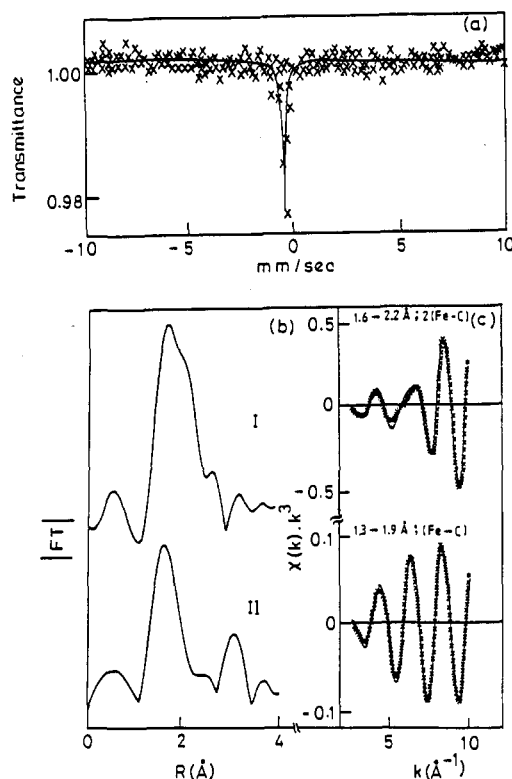


**Figure 2.**  $^{57}\text{Fe}$  Mössbauer spectrum of  $\text{FeC}_{60}$  (I) (a); Fourier transforms of the Fe-K EXAFS of  $\text{FeC}_{60}$  (I and II) (b); inverse-transformed EXAFS data (c).

the half-mass of  $\text{FeC}_{60}$ . The presence of peaks due to  $\text{C}_2$  and  $\text{C}_4$  losses in the decreasing order of intensity suggests that Fe may be internally bound to the  $\text{C}_{60}$  frame. Similar  $\text{C}_2$  losses found in  $\text{HeC}_{60}$  and  $\text{LaC}_{60}$  have been attributed to the entrapment of He and La in the hollow cage.<sup>5,6</sup> The  $^{57}\text{Fe}$  Mössbauer spectrum<sup>9</sup> of the adduct<sup>12</sup> shows a singlet with an isomer shift of  $-0.083$  mm/s with respect to  $\alpha\text{-Fe}$  (Figure 2a), characteristic of iron in a near-zero oxidation state. The sharpness of the spectrum suggests a strongly bound Fe species. The compound was paramagnetic over the 10–300 K range, and its electronic absorption spectrum showed a slight red shift relative to that of  $\text{C}_{60}$ . The IR spectrum showed little change from that of  $\text{C}_{60}$ .

Unlike the  $\text{FeC}_{60}$  (I) prepared by the gas-phase reaction, solid  $\text{FeC}_{60}$  (II) where Fe was bound externally to the fullerene<sup>13</sup> showed a doublet in the Mössbauer spectrum with an isomer shift of 0.45 mm/s due to Fe(III); magnetic susceptibility measurements

(12) The sample gave a single spot in TLC and satisfactory analysis for Fe (7.2%) and C (92%). A preliminary study of the powder X-ray diffraction pattern of  $\text{FeC}_{60}$  (I) suggests that a primitive tetragonal structure ( $a = 15.43$  Å,  $c = 9.08$  Å) may be preferable over the FCC structure. The strongest (221) reflection could be simulated with Fe atoms in the cage 8 Å apart.

(13) The solid Na compound of  $\text{C}_{60}$  prepared by the reaction of Na with  $\text{C}_{60}$  in toluene solution was reacted with  $\text{FeCl}_2$  in THF solution to obtain solid  $\text{FeC}_{60}$  (anal. Fe 7.2%).

showed evidence for antiferromagnetic interaction. Both the electronic and infrared spectra were different from those of  $\text{C}_{60}$ . Furthermore, the mass spectrum did not show  $\text{C}_2$  losses.<sup>14</sup>

We have examined the structures of the two  $\text{FeC}_{60}$  adducts (I and II) by means of Fe-K EXAFS measurements by employing a Rigaku spectrometer. Figure 2b shows the Fourier transforms of the EXAFS data obtained with  $k_{\text{min}} 3.0$  and  $k_{\text{max}} 12.0$  Å<sup>-1</sup> after weighing the data by  $k^3$ . Analysis of the EXAFS data, including curve fitting of the inverse-transformed data (employing ferrocene as the reference), gave a good fit (Figure 2c) with two coordinations for Fe at Fe–C distances of 2.06 and 2.34 Å for  $\text{FeC}_{60}$  (I) with lower Debye–Waller factors ( $\Delta\sigma^2 = 0.0002$  Å<sup>2</sup>). Two such short Fe–C distances can only be reconciled if Fe is in the cage. Any adduct with Fe bound externally would show a single short Fe–C distance, as indeed found by us from the analysis of the EXAFS of  $\text{FeC}_{60}$  (II) prepared from solution reaction (Figure 2b). In this solid, where Fe is externally bound, we find Fe–C distances of 2.03 and 3.46 Å with  $\Delta\sigma^2$  of 0.0003 and 0.001 Å<sup>2</sup>, respectively.

The near-zero oxidation state of Fe,  $\text{C}_2$  losses in the mass spectrum, the occurrence of the two Fe–C distances close to each other, as well as some of the other features indicate that  $\text{FeC}_{60}$  (I) obtained by the gas-phase reaction during arc vaporization of graphite is likely to be an endohedral species with the Fe atom inside the cage of  $\text{C}_{60}$ . Further studies on the various  $\text{FeC}_{60}$  adducts are in progress.

**Registry No.**  $\text{Fe}^1\text{C}_{60}$ , 137433-48-8;  $\text{Fe}(\text{CO})_5$ , 13463-40-6;  $\text{C}_{60}$ , 99685-96-8;  $\text{FeCl}_2$ , 7758-94-3;  $\text{NaC}_{60}^+$ , 137718-24-2; Na, 7440-23-5; graphite, 7782-42-5.

(14) We have sought to prepare  $(\text{C}_{60})_2\text{Fe}$  by reacting the monosodium salt of  $\text{C}_{60}$  with  $\text{FeCl}_2$  in THF solution. A brown solid thus obtained has a different electronic spectrum. Electron-impact mass spectroscopy unfortunately seems to fragment the species. Fe–C distances in this ferrocene analogue cannot be distinguished from those of  $\text{FeC}_{60}$  (II).

## Nanoarchitectures. 1. Controlled Synthesis of Phenylacetylene Sequences

Jinshan Zhang, Jeffrey S. Moore,\* Zhifu Xu, and Ryan A. Aguirre†

The Willard H. Dow Laboratories  
Department of Chemistry and the Macromolecular  
Research Center, The University of Michigan  
Ann Arbor, Michigan 48109-1055

Received November 14, 1991

Well-defined oligomeric sequences are valuable models for investigating how physical properties depend on molecular size and chemical structure. For example, controlled sequences have recently been used to study cooperative motions<sup>1</sup> and microphase separation<sup>2</sup> of copolymers. Monodisperse sequences have also been used to study the electronic properties of conjugated chains, such as optical nonlinearity<sup>3</sup> and band gap.<sup>4</sup> We have found that well-defined oligomers are valuable for preparing very large two- and three-dimensional molecular frameworks.<sup>5</sup> Outside the realm

\* Participant in the NSF Research Experience for Undergraduates program.

(1) Jho, J.; Yee, A. F. *Macromolecules* 1991, 24, 1905.  
(2) Wagener, K. B.; Matayabas, J. C.; Wanigatunga, S. *Macromolecules* 1989, 22, 3211.

(3) (a) Huijts, R. A.; Hesselink, G. L. *J. Chem. Phys. Lett.* 1989, 156, 209.  
(b) Barzoukas, M.; Blanchard-Desce, M.; Josse, D.; Lehn, J.-M.; Zyss, J. *Chem. Phys.* 1989, 133, 323.

(4) (a) ten Hoeve, W.; Wynberg, H.; Havinga, E. E.; Meijer, E. W. *J. Am. Chem. Soc.* 1991, 113, 5887. (b) Khanna, R. K.; Jiang, Y. M.; Creed, D. J. *Am. Chem. Soc.* 1991, 113, 5451. (c) Knoll, K.; Schrock, R. R. *J. Am. Chem. Soc.* 1989, 111, 7989.

(5) Moore, J. S.; Zhang, J.; Wu, Z. Unpublished results.